Research Square

Preprints are preliminary reports that have not undergone peer review.
They should not be considered conclusive, used to inform clinical practice,
or referenced by the media as validated information.

Temporal preparation in rats: Evidence from a variable foreperiod paradigm and shifted Wald modeling

Fatemeh Mafi
Kerman University of Medical Sciences
Mohammad Reza Afarinesh
Kerman University of Medical Sciences
Vahid Sheibani
Kerman University of Medical Sciences
Sadegh Ghasemian
s.ghasemian1975@gmail.com

Kerman University of Medical Sciences

Article

Keywords: temporal preparation, variable foreperiod, shifted Wald, distribution effect, transfer effect

Posted Date: November 25th, 2026

DOI: https://doi.org/10.21203/rs.3.rs-11156167/v1

License: This work is licensed under a Creative Commons Attribution 4.0 International License.
Read Full License

Additional Declarations: No competing interests reported.

Abstract

Temporal preparation—the ability to anticipate when events will occur—is fundamental to adaptive behavior. While extensively studied in humans, evidence for the full family of foreperiod (FP) effects in rodents remains scarce. Here, we developed a self-paced simple reaction time task in rats (N = 10) to examine four temporal preparation effects within a single paradigm: current-trial FP, sequential, distribution, and transfer effects. FPs varied randomly (200–800 ms) across uniform, exponential, and anti-exponential distributions. We applied Bayesian shifted Wald modeling to decompose reaction times into latent cognitive components: drift rate (evidence accumulation), threshold (response caution), and non-decision time. Results revealed a robust current-trial FP effect driven by both reduced threshold and increased drift rate. Sequential effects were weak and confined to threshold. Distribution effects were parameter-specific: anti-exponential reduced drift rate and attenuated its FP modulation, while exponential reduced threshold without affecting drift. Transfer effects mirrored these patterns: exponential pretraining attenuated the RT-FP slope, whereas anti-exponential pretraining reduced baseline drift without modulating the slope. Parameter recovery simulations confirmed that non-decision time was not reliably identifiable when allowed to vary with FP. These findings demonstrate that rats exhibit a subset of human temporal preparation effects, with computational mechanisms distributed across decision-related parameters. The results support the rodent as a translational model for investigating the cognitive and neural architecture of temporal preparation.

1. Introduction

Time is a pervasive dimension of behavior. Organisms can learn temporal regularities and adjust their actions based on when events are likely to occur, tuning their readiness for upcoming events through a process known as temporal preparation (Bausenhart & Ulrich, 2026; Niemi & Näätänen, 1981; Salet, 2023; Salet, Kruijne, van Rijn, et al., 2022). Rather than merely tracking elapsed intervals, individuals extract statistical regularities from their temporal environment and use these regularities to optimize performance (Salet, Kruijne, Rijn, et al., 2022). A foraging rat that hears rustling vegetation—a sound that reliably precedes a predator's strike within seconds—gradually increases its defensive preparedness as the probable moment of danger approaches. This dynamic adjustment illustrates how temporal expectations, derived from the statistical structure of environmental cues, enhance behavioral readiness. Such learning-based, time-dependent adjustments have been extensively documented in humans as a family of experimental phenomena, particularly in the context of variable foreperiod (FP) paradigm (Los et al., 2021; Mattiesing et al., 2017; Niemi & Näätänen, 1981). However, the generalizability of these effects across species and the potential cognitive mechanisms that underlie them in the framework of sequential sampling models remains poorly understood (Salet, Kruijne, van Rijn, et al., 2022).

Experimental paradigms that manipulate foreperiods (FPs)—the intervals between a warning and an imperative stimulus—have been widely used to study temporal preparation (Niemi & Näätänen, 1981). Depending on time scale, several preparation effects have been reported, specifically with the variable FP paradigm, where FPs vary randomly across trials. The first effect is a within-trial effect, whereby the

length of FP has a negative correlation with reaction time (RT); producing the classic variable foreperiod effect (Los, 2010). The second effect is a between-trial sequential effect, manifested as increased RT when the current FP is shorter than the preceding FP, but unchanged when it is longer, reflecting an asymmetric influence of previous trials on temporal preparation (Capizzi et al., 2015; Los, 2010). The third effect occurs across trials and arises from the distribution of FPs within an experimental block. In an anti-exponential block, long FPs occur more frequently than in a uniform block, whereas an exponential block contains more short FPs. The RT–FP function is steeper under the anti-exponential distribution than under the uniform distribution, while it is a nearly flat function under the exponential distribution (Los et al., 2017). The fourth effect is a transfer effect, which occurs across experimental blocks. Specifically, in a test phase with a uniform FP distribution, the RT–FP function tends to resemble the function derived from the distribution used during the acquisition phase (Crowe et al., 2021; Mattiesing et al., 2017).

Several theoretical frameworks have been proposed to explain this family of phenomena. Hazard-based models (Janssen & Shadlen, 2005; Nobre et al., 2007; Vangkilde et al., 2013) posit that the brain continuously estimates the conditional probability of target occurrence over time—the hazard rate—which can increase, decrease, or remain constant depending on the FP distribution. Although these models can reasonably explain the main current-trial FP and distribution effects, they fail to explain asymmetric sequential effects and transfer effects. In contrast, memory-based accounts such as the multiple trace theory of temporal preparation (Los et al., 2014) and its formalized computational implementation fMTP (Salet, Kruijne, van Rijn, et al., 2022) propose that each experienced FP leaves a memory trace encoding preparatory activation and inhibition dynamics. These traces accumulate over time and jointly determine performance on subsequent trials, providing a unified account of short-term sequential effects, intermediate-scale FP effects, and long-term transfer effects. Despite the success of memory-based accounts in explaining the full range of temporal preparation effects, the computational mechanisms behind these effects remain largely under-explored, specifically for sequential, distribution, and transfer effects (Salet, Kruijne, van Rijn, et al., 2022).

Although humans have been studied extensively in variable FP tasks, comparatively little is known about temporal preparation effects in non-human animals. Studies in monkeys have documented the variable FP effect across different paradigms (Borzadaran et al., 2025; Brulé et al., 2021; de Hemptinne et al., 2007; Ilhame et al., 2015; Oláh et al., 2020; Tsuchiya et al., 2025). However, other temporal preparation effects remain under-explored. For example, the sequential effect was lacking in an arm-reaching task (Pasquereau & Turner, 2015), while other study has found that its influence may be context dependent, affecting primarily response inhibition processes rather than simple reaction times in a stop-signal task (Borzadaran et al., 2025). The distribution effect has also been revealed in monkeys (Tsunoda & Kakei, 2008), but evidence regarding the transfer effect—the carryover of learned temporal expectations across different FP distributions—is generally lacking. These findings highlight both cross-species similarities in temporal learning and potential differences in short-term adaptive mechanisms. In rats, the variable FP effect has been robustly demonstrated using simple reaction time tasks (Hauber et al., 2001; Narayanan et al., 2006; O'Neill & Brown, 2007) and a rodent version of the psychomotor vigilance test (Davis et al.,

2016). However, evidence for other temporal preparation effects—including sequential, distribution, and transfer effects—remains scarce in the rodent literature, leaving important questions open regarding the generality of these phenomena across species.

Rodents offer critical advantages for uncovering the neural substrates of temporal preparation: their shorter generation time, well-characterized neuroanatomy, and extensive toolbox for optogenetic, chemogenetic, and electrophysiological recording enable causal testing of circuits implicated in temporal expectancy—experiments that are often infeasible in humans and logistically challenging in monkeys. Moreover, establishing that rats exhibit the same family of foreperiod effects as humans would validate the rodent as a translational model for studying the cognitive and neural mechanisms of temporal preparation, and would help disentangle which aspects of these effects are phylogenetically conserved versus species-specific.

Sequential sampling models of decision making decompose RT into latent cognitive components such as evidence accumulation rate (drift rate), decision threshold, and non-decision time, revealing which processing stage is modulated by experimental manipulations. In both fixed foreperiod and temporal cueing paradigms, the Ratcliff diffusion model and the shifted-Wald model have consistently revealed that temporal expectation primarily affects non-decision processes (target encoding and/or response preparation) rather than decision threshold or drift rate (Jepma et al., 2012). Other studies with constant foreperiod tasks also suggest that temporal preparation leads to earlier evidence accumulation, as revealed by speed–accuracy trade-off analysis (Bausenhart et al., 2010), decision criterion model (Seibold et al., 2011) and ex-Gaussian distribution of RT (Leth-Steensen, 2009). Furthermore, in Parkinson's disease patients, impaired temporal preparation under dopaminergic depletion has been linked to an inflexibly high decision threshold in a variable foreperiod task (Tomassini et al., 2019). In the somatosensory domain, temporal expectation shortens non-decisional processes but reduces the rate of evidence accumulation (Xiong et al., 2025). Similarly, in a visual detection task with temporal cueing, temporal expectation has been associated with shorter non-decision time but preserved evidence accumulation (van den Brink et al., 2021). Regarding the transfer effect, drift rate appears to be the most sensitive parameter, with exposure to temporal variability affecting evidence accumulation in the transfer phase (Shdeour et al., 2024). Thus, the origin of temporal preparation effects in sequential sampling models does not reveal a single clear pattern; instead, it suggests a flexible adjustment of multiple parameters depending on the temporal structure of the task and the predictability of the target.

Here, we developed a self-paced simple RT task to examine the presence of different temporal preparation effects in rats. For computational modeling of these effects, we applied a Bayesian shifted Wald modeling framework to capture the full distribution of RTs, including mean responses and slow tails sensitive to temporal expectations and prior learning. The shifted Wald model offers a principled approach for understanding the cognitive processes underlying single-choice decisions (Anders et al., 2016). This distribution formalizes RTs as arising from a stochastic evidence accumulation process toward a single threshold, combined with a shift parameter that captures non-decision components. In the classic parametrization of the shifted Wald model, three parameters govern the RT distribution: the

drift rate (γ) quantifies the average speed of evidence accumulation, reflecting processing efficiency; the threshold (α) represents the amount of evidence required to trigger a response, indexing response caution or decisiveness; and the non-decision time (θ) isolates the duration of perceptual and motor stages, separating them from the core decision process (Heathcote, 2004; Matzke & Wagenmakers, 2009). Because the present task involves rapid, low-error, single-choice responses, the shifted Wald model is particularly well suited: it captures the full RT distribution and separates accumulation rate, threshold, and non-decision time without requiring the joint modeling of accuracy. At the same time, this advantage also implies a limitation: the model cannot jointly account for error rates, making low error rates essential for valid inference.

Here, we addressed two questions. First, do rats exhibit the full family of temporal preparation effects—current-trial FP, sequential, distribution, and transfer effects—within a single variable-FP paradigm? Second, which latent cognitive components mediate these effects? To address these questions, we developed a self-paced simple RT task in rats, in which FPs varied across trials and blocks, allowing us to assess all four effects within the same animals. We fitted hierarchical Bayesian shifted Wald models to single-trial RT distributions to decompose performance into drift rate (γ), threshold (α), and non-decision time (θ). Regarding the computational locus of temporal preparation effect, if temporal preparation primarily tunes response readiness, non-decision time should vary with FP; if it alters evidence accumulation, drift rate should track distribution and transfer; and if it modulates response caution, threshold should vary. By identifying which parameters capture each effect in rats, this work will establish the rodent as a translational model for temporal preparation and clarify which computational mechanisms are conserved across species.

2. Materials and Methods

2.1. Animals

Twelve Wistar rats (7 female, 5 male), weighing 180–200 g at the start of the study, were used. Two rats (1 female) were excluded from data analysis due to poor task engagement and unstable performance. Animals were purchased from animal farm of Kerman University of Medical Sciences. At the beginning of training, rats were 6–8 weeks old, and at the time of testing, they were 3–4 months old. Animals were housed under a 12-h light–dark cycle (lights off at 19:00 h). Food was available *ad libitum*, and water was provided for 2 h daily immediately after each training or testing session. All experiments were performed in accordance with the Guide for the Care and Use of Laboratory Animals (Albus, 2012) and approved by the Ethics Committee of Kerman University of Medical Sciences.

2.2. Apparatus

Behavioral training and testing were conducted in a custom-made wooden operant chamber (35 cm × 25 cm × 35 cm) inside a sound-attenuating chamber. The front wall of the operant chamber contained a central nose-poke aperture (1.5 cm depth) positioned 4 cm above the floor. A reward spout was located 5 cm above the nose-poke aperture, adjacent to a 5 mm white light-emitting diode (LED) that served as

imperative signal. Reward (5% sucrose solution) was delivered upon each completed trial via a solenoid valve. A second white LED, positioned behind the nose-poke aperture, served as warning signal. The rear wall of the nose-poke area was transparent, allowing animals visual access to the warning signal. Both the spout and the nose-poke aperture were equipped with infrared proximity sensors to detect licking and nose-poking, respectively. All experimental events were controlled by a custom MATLAB script interfaced with an Arduino board. During training and testing sessions, the chamber was illuminated with a 9 W red LED bulb to enable video monitoring.

2.3. Behavioral task and procedures

Rats were trained and tested on a simple choice reaction time task incorporating a variable foreperiod (FP)—the delay between warning signal offset and presentation of an imperative signal (Fig. 1). Each trial began with the illumination of a white LED located behind the nose-poke aperture (i.e., warning signal), signaling that the aperture was active. Upon insertion of the nose into the aperture, this LED was turned off, and the FP commenced. The FP duration was randomly selected on each trial from four possible delays: 200, 400, 600, or 800 ms. During the FP, rats were required to maintain their nose into the aperture (hold period). Premature withdrawal from the aperture before imperative cue onset resulted in trial termination with no reward, followed by a 3 s inter-trial interval (ITI). Following a successful hold (i.e., the rat remained in the aperture for the entire FP), an imperative visual stimulus (white LED located above the nose-poke aperture, adjacent to the reward spout) was turned on. In response, the rat was required to release the hold and lick the spout. Complete responses were immediately followed by reward and the onset of the ITI. This self-paced design was intended to enhance the animals' attention to FP duration.

The first aim of the study was to examine the effects of variable FP and sequential trial history on reaction time (RT). To address this aim, data were collected across multiple sessions (5–8 sessions per rat). Each session consisted of 240 trials with a uniform distribution of the four FP durations (60 trials per FP).

The second aim was to investigate how the distribution of FP durations modulates the RT–FP function (i.e., the variable foreperiod effect). Two non-uniform distributions were applied in alternating sessions: exponential and anti-exponential. In exponential block (105 trials total), the 200, 400, 600, and 800 ms FPs were presented with relative frequencies of 8, 4, 2, and 1, respectively. In anti-exponential block, the respective frequencies were reversed (1, 2, 4, and 8).

The third aim was to assess transfer effects—specifically, how prior training with different FP distributions influences the variable foreperiod effect in subsequent test block. Testing block (160 trials) employed a uniform distribution of FP durations and were introduced 5 minutes after the completion of each training block.

2.4. Data analysis

The data were analyzed in a Bayesian framework using two complementary approaches: first, a hierarchical linear regression to characterize observed RT patterns, and second, a shifted-Wald (SW) decomposition to infer the latent decision processes. Only RTs between 50 and 3000 ms were included in analyses.

Observed RTs were first analysed using a non-hierarchical (pooled) Bayesian linear regression with fixed intercepts and slopes estimated across all rats. The model included current FP as the primary continuous predictor. For analyses examining sequential effects, history FP (the FP of the preceding (n-1) trial) and its two-way interaction with current FP were also included as predictors. In separate analyses investigating distribution and transfer effects, the distribution of FPs (uniform, anti-exponential, exponential) and the distribution of FPs in the training phase were included as categorical predictors alongside the current FP. All continuous predictors were mean-centered to facilitate interpretation of effects. Weakly informative Normal and HalfNormal priors were assigned to all regression coefficients and standard deviation parameters, allowing the data to dominate the posterior estimates.

To examine RTs within a process-level framework, we applied the Shifted Wald (SW) distribution, which is appropriate for single-choice decision tasks and decomposes each RT into three latent components: drift rate (γ; speed of evidence accumulation), decision threshold (α; response caution), and non-decision time (θ; encompassing sensory and motor delays). The SW distribution was parameterized with mean $\mu = \alpha / \gamma$, shape $\lambda = \alpha^2$, and shift θ. All parameters were modelled using a log-link function, ensuring positivity while allowing multiplicative effects of predictors on the original scale.

A critical prerequisite for meaningful inference is parameter identifiability. Preliminary parameter recovery simulations revealed that allowing θ to vary with FP produced unreliable estimates for θ slope (see Results for details). Consequently, we treated θ as a constant parameter in all subsequent analysis concerning sequential, distribution and transfer effects, focusing inference on the decision-related parameters α and γ. All models were non-hierarchical (pooled), with fixed intercepts and slopes estimated across all rats. Weakly informative Normal priors were placed on the log-scale intercepts and slopes.

In separate analysis of sequential, distribution and transfer effects, we aimed at determining which decision parameters were influenced by the experimental manipulations. For each analysis, we compared three nested models: one allowing only α to vary with predictors, one allowing only γ to vary, and one allowing both to vary. All models were estimated in a Bayesian framework using the No-U-Turn sampler (NUTS) with four chains of 3000 warmup and 2000 samples each. Convergence was assessed by visual inspection of trace plots and by ensuring that all potential scale reduction factors ($\hat{R}$) were below 1.01. Posterior predictive checks were performed for the selected model to evaluate its descriptive adequacy. Model comparison was conducted using approximate leave-one-out cross-validation (LOO-CV) with the expected log pointwise predictive density (elpd_loo) as the selection criterion. The model with the highest elpd_loo was retained as the best-fitting model for presentation of findings for each effect.

3. Results

We adopted the SW model, which decomposes RT into decision-related processes (threshold and drift rate) and a non-decision component (shift), allowing us to test whether FP effects are primarily driven by changes in decision processes, non-decision processes, or both. A critical prerequisite for such inference is parameter identifiability; we therefore conducted a comprehensive assessment combining model comparison with parameter recovery simulations. Here, we first present the results of the model comparison and parameter recovery to establish the identifiability of the best candidate models. We then proceed to examine the effects of our experimental manipulations—sequential effects, distribution effects, and transfer effects—using model comparison for each effect.

3.1. Parameter identifiability of variable foreperiod effect in the shifted Wald model

To assess the appropriateness of the SW model for the variable FP effect, we compared seven candidate models using LOO-CV (See supplementary table S1 online for details on model specifications and comparison metrics). The full model, which allowed all three parameters (α, γ, and θ) to vary with FP, was strongly favored (ELPD = 543.25, SE = 106.16), outperforming the next best model, alpha-gamma (ELPD = 531.56, ΔELPD = 11.69, SE_diff = 5.09), which only allowed α and γ to vary with FP. Models omitting FP effects on α or γ performed considerably worse (ΔELPD ≥ 54.12), while the theta-only model was by far the worst (ΔELPD = 941.21). Posterior predictive checks revealed that both the full and alpha-gamma models reasonably reproduce the pattern of reaction time across FPs (supplementary Fig. S1 & S2 online).

From the full model, the baseline estimates (at mean FP) on the log scale were: α_0 = 0.773 (95% HDI: 0.752–0.794), γ_0 = 1.162 (95% HDI: 1.147–1.177), and θ_0 = − 4.726 (95% HDI: − 5.199 to − 4.250). The baseline non-decision time on the original scale was $\exp(\theta_0) \approx 8.8$ ms (95% HDI: 5.5–14.2 ms), which is extremely short. Each 1-second increase in FP reduced the decision threshold by 41.0% (β = − 0.528, 95% HDI: − 0.612 to − 0.435), increased the drift rate by 39.6% (β = 0.334, 95% HDI: 0.273–0.393), and increased the non-decision time (β = 4.172, 95% HDI: 2.893–5.406; corresponding to a ~ 65-fold increase). However, the wide HDI for θ slope (18- to 223-fold) suggested substantial uncertainty in its magnitude. In the alpha-gamma model (θ constant), the baseline estimates on the log scale were: α_0 = 0.807 (95% HDI: 0.794–0.820), γ_0 = 1.176 (95% HDI: 1.163–1.189), and θ_0 = − 6.094 (95% HDI: − 7.011 to − 5.175). The baseline non-decision time on the original scale was $\exp(\theta_0) \approx 2.2$ ms (95% HDI: 0.9–5.6 ms). Similar to the full model such values for non-decision time are extremely short and implausible. The decision threshold decreased by 31.3% per 1-second increase in FP (β = − 0.375, 95% HDI: − 0.425 to − 0.330), while the drift rate increased by 48.3% (β = 0.394, 95% HDI: 0.343–0.448).

To determine whether the full model's θ slope could be reliably estimated, we conducted a parameter recovery study for both models. True parameters were drawn from the posterior of the respective models, used to generate synthetic datasets, and then re-fitted with the same model. Across 200

iterations, recovery was assessed via correlation, bias, RMSE, and coverage (the proportion of iterations where the true parameter fell inside the 95% HDI of the recovered posterior).

For the full model, the FP effects on decision threshold (r = 0.65, coverage = 0.91) and drift rate (r = 0.67, coverage = 0.96) were reasonably recovered with small biases (≤ 0.01 on the log scale). The intercepts α_0, γ_0, and θ_0 also showed acceptable recovery (coverage ≥ 0.43). In stark contrast, the FP effect on θ showed catastrophic recovery: coverage was only 0.02 (the true value fell inside the 95% HDI in only 2% of iterations), with a massive negative bias of − 2.58 (log scale) and high RMSE (2.68). The true log-scale mean was 4.13, but the recovered mean was only 1.55, indicating severe underestimation. See supplementary table S2 online for full details of parameter recovery results and supplementary Fig. S3 online for plots of observed versus mean recovered values. This implies that although the full model had the highest LOO score, its superior predictive performance is driven by a parameter that cannot be reliably recovered.

In the alpha-gamma model, the threshold slope (r = 0.67, coverage = 0.84) and drift slope (r = 0.68, coverage = 0.94) were also reasonably recovered with small biases (≤ − 0.02 on the log scale). The θ_0 was poorly recovered (coverage = 0.22, large positive bias). See supplementary table S2 online for full details and supplementary Fig. S4 online for plots of observed versus mean recovered values. The θ is treated as a constant parameter and its absolute value is not of primary theoretical interest, therefore the poor recovery of the intercept does not affect the interpretability of the FP effects on α and γ. Parsimony and identifiability outweigh a modest predictive gain. The full model's unidentifiable θ slope undermines any interpretation of FP effect on non-decision time. Therefore, all candidate models allowing a θ slope for any experimental manipulation were excluded from model comparisons in subsequent analyses concerning sequential, distribution, and transfer effects. As a result, model comparison was restricted to three possible models: alpha-only, gamma-only, and alpha-gamma.

3.2. Foreperiod sequential effects on reaction time and decision parameters

3.2.1. Reaction time

Reaction times were analyzed using a Bayesian hierarchical linear model with current FP, history FP, and their interaction as continuous predictors. Convergence diagnostics were excellent, with all $\hat{R} \leq 1.001$ and effective sample sizes (ESS > 7700), indicating highly stable posterior estimates.

The current FP effect was robust: longer FPs were strongly associated with faster RTs (β = − 0.540, 95% HDI: − 0.558 to − 0.522), confirming the canonical variable foreperiod effect, which is a typical effect in paradigms with variable FP (Fig. 2a). The main effect of history FP was small but reliable, with longer preceding FPs leading to slightly slower RTs (β = 0.023, 95% HDI: 0.004 to 0.040). The interaction between current and history FPs was negative (β = − 0.190, 95% HDI: − 0.270 to − 0.107), indicating that the facilitatory effect of a longer current FP was amplified when the history FP was also long, rather than short. Collectively, these results demonstrate a robust current FP effect, a modest yet reliable influence

of previous trial history, and a meaningful sequential effect in which the magnitude of the current FP benefit is modulated by the preceding FP (Fig. 2a).

3.2.2. Shifted Wald model

Model comparison was performed between three candidate models: the alpha-gamma model, which allowed α and γ to vary with current FP, history FP, and their interaction; the alpha-only model, which allowed only α to vary; and the gamma-only model, which allowed only γ to vary. The alpha-gamma model was strongly favored (ELPD = 538.89), substantially outperforming alpha-only (ELPD = 435.97, ΔELPD = 102.92) and gamma-only (ELPD = 424.54, ΔELPD = 114.35). These results indicate that both threshold and drift rate are required to account for the data, while allowing only one of them to vary with predictors is insufficient.

The selected model showed excellent convergence (all $\hat{R} \leq 1.001$) and large effective sample sizes (ESS > 5000 for all parameters), indicating highly reliable posterior estimates. For drift rate, the current FP had a clear positive effect (β = 0.401, 95% HDI: 0.349 to 0.457), indicating faster evidence accumulation with longer FPs (Fig. 2b). The main effect of history FP was small and not credible (β = 0.030, 95% HDI: − 0.025 to 0.087), and the interaction between current and history FPs was also not credible (β = 0.133, 95% HDI: − 0.121 to 0.373). Thus, drift rate was influenced only by the current FP, with no evidence of sequential modulation.

For threshold, the current FP revealed a robust negative effect (β = − 0.362, 95% HDI: − 0.413 to − 0.314), reflecting reduced response caution with longer FPs (Fig. 2c). The history FP showed a small positive effect that was credible (β = 0.060, 95% HDI: 0.011 to 0.108), suggesting that response threshold increased with increasing FP in the previous trial. The current FP × history FP revealed no credible effect (β = − 0.075, 95% HDI: − 0.296 to 0.155). These results indicate that response caution was primarily determined by the current FP, with a modest influence from the preceding trial.

The alpha-gamma model could reasonably reproduce the pattern of observed RTs (Fig. 2d) and confirms that the variable FP effect on RT is driven by both a reduction in decision threshold and an increase in drift rate, while sequential effects from the previous trial are weak and mainly affect response caution regardless of FP in the current trial.

3.3. Foreperiod distribution effects on reaction time and decision parameters

3.3.1. Reaction time

A Bayesian linear regression examined the effects of FP and block-wise distribution of FPs (uniform, anti-exponential, exponential) on RT. The model was fitted with four MCMC chains; convergence diagnostics were excellent, with $\hat{R} \leq 1.001$ and ESS > 4300 for all parameters. There was strong evidence for a negative main effect of FP (β = − 0.539, 95% HDI: − 0.567 to − 0.511), indicating that RT decreased as FP increased. Relative to the uniform distribution, the anti-exponential distribution showed a small but

credible increase in average RT (β = 0.017, 95% HDI: 0.004 to 0.030), meaning that RTs in the anti-exponential condition were slightly slower than those of the uniform condition. In contrast, the exponential distribution produced significantly faster average RTs (β = − 0.097, 95% HDI: − 0.110 to − 0.085), compared to uniform distribution (Fig. 3a). Critically, the interaction between FP and distribution revealed credible evidence that the slope of the RT–FP function was attenuated in the anti-exponential compared to the uniform distribution (β = 0.124, 95% HDI: 0.073 to 0.174). For the exponential distribution, the interaction was also credible (β = 0.081, 95% HDI: 0.030 to 0.128), indicating that the FP effect was also attenuated relative to uniform, though to a lesser extent. Overall, these results indicate that FP strongly speeds RT regardless of distribution, but the distribution modulates the magnitude of this FP effect: anti-exponential distributions flatten the RT–FP slope relative to uniform, while the exponential distribution produces a less pronounced flattening.

3.3.2. Shifted Wald model

Similar to the modeling approach for the sequential effect, a set of three candidate models was fitted to the data. The model comparison clearly identified the alpha-gamma model as the best fitting description of the data (ELPD = − 181.67). The alpha-only model performed substantially worse (ELPD = − 303.26), with a difference of 121.59 from the best-fitting model. The gamma-only model provided a very poor fit (ELPD = − 326.37), with a difference of 144.70. These results demonstrate that both decision threshold and drift rate are sensitive to FP distribution.

The alpha-gamma model showed excellent convergence (all $\hat{R} \leq 1.002$ and ESS > 2900 for all parameters). The current FP had a clear positive effect on drift rate (β = 0.489, 95% HDI: 0.403 to 0.570), indicating that evidence accumulation increased with increasing FP. Relative to the uniform distribution, drift rate was substantially lower for the anti-exponential distribution (β = − 0.180, 95% HDI: − 0.219 to − 0.139), while the exponential distribution did not differ credibly from uniform (β = 0.023, 95% HDI: − 0.016 to 0.057). The interaction between current FP and anti-exponential distribution was credible (β = − 0.170, 95% HDI: − 0.315 to − 0.012), indicating that the FP effect on drift rate was attenuated for the anti-exponential distribution (Fig. 3b). The interaction with exponential distribution was not credible (β = − 0.048, 95% HDI: − 0.198 to 0.094). Thus, while drift rate was modulated by both current FP and distribution type, the FP effect on drift rate differed only for the anti-exponential distribution.

Regarding the threshold, current FP revealed a robust negative effect (β = − 0.284, 95% HDI: − 0.355 to − 0.209), reflecting reduced response caution with longer FPs (Fig. 3c). Relative to the uniform distribution, threshold was lower for both the anti-exponential (β = − 0.148, 95% HDI: − 0.182 to − 0.114) and the exponential (β = − 0.123, 95% HDI: − 0.154 to − 0.092) distributions. Interactions between current FP and distribution type were not credible: current FP × anti-exponential (β = 0.009, 95% HDI: − 0.123 to 0.139) and current FP × exponential (β = − 0.015, 95% HDI: − 0.143 to 0.111). These findings indicate that response caution was reduced for both non-uniform distributions relative to uniform, with the anti-exponential distribution showing a slightly larger reduction, but the FP effect on threshold remained comparable across distributions.

The model reasonably predicted the pattern of RTs across distributions and FPs (Fig. 3d), These findings indicate that FP distribution systematically modulates both parameters: the anti-exponential distribution produces slower drift (and attenuates the FP effect on drift) and lower threshold compared to uniform, while the exponential distribution reduces threshold without affecting drift rate or its FP modulation.

3.4. Foreperiod distribution transfer effects on reaction time and decision parameters

3.4.1. Reaction time

A Bayesian linear regression examined the effects of FP and pretraining distribution (uniform, anti-exponential, exponential) on reaction time in the test phase (uniform FP distribution). The convergence diagnostics were excellent ($\hat{R} \leq 1.001$ and ESS > 3000 for all parameters). There was strong evidence for a robust variable FP effect ($\beta = -0.547$, 95% HDI: − 0.571 to − 0.524), indicating that RT decreased with increasing FP. Relative to pretraining with uniform distribution (reference), the anti-exponential pretraining condition produced slightly slower average RTs ($\beta = 0.013$, 95% HDI: 0.005 to 0.022), whereas the exponential pretraining condition produced faster overall RTs ($\beta = -0.039$, 95% HDI: − 0.047 to − 0.031). The interaction between FP and pretraining distribution was credible for the exponential condition ($\beta = 0.085$, 95% HDI: 0.051 to 0.117), indicating that the RT–FP slope was attenuated (i.e., shallower) in the exponential pretraining condition relative to the uniform condition. For the anti-exponential condition, the interaction was not credible ($\beta = 0.025$, 95% HDI: − 0.012 to 0.059), suggesting that the FP slope did not differ reliably between the anti-exponential and uniform pretraining (Fig. 4a). Overall, these results indicate a transfer effect: prior exposure to the exponential distribution attenuates the variable FP effect, while prior exposure to the anti-exponential distribution produces slower overall RTs without reliably modulating the RT-FP slope.

3.4.2. Shifted Wald model

To examine how transfer effects emerge at the parameter level, a set of candidate models was fitted to reaction times. The current FP and pretraining distribution (uniform, exponential, anti-exponential), as well as their interaction, were included as predictors. Following the simplified modeling approach, three candidate models were compared: alpha-only, gamma-only, and alpha-gamma. LOO-based comparison decisively revealed the alpha-gamma model (ELPD = − 71.49) as the best-fitting model, in which both decision threshold and drift rate varied with FP, pretraining distribution, and their interaction. The gamma-only model performed substantially worse (ELPD = − 450.17), with a difference of 378.69 from the best model. The alpha-only model provided an extremely poor fit (ELPD = − 1057.18), with a difference of 985.70. These comparisons demonstrate that transfer effects of pretraining distribution are expressed across multiple latent decision parameters rather than a single component, with both evidence accumulation (γ) and response caution (α) contributing to predictive accuracy.

The alpha-gamma model showed excellent convergence (all $\hat{R} \leq 1.002$) and large effective sample sizes (ESS > 2900 for all fixed effects), indicating reliable posterior estimates. For drift rate, the current FP had

a clear positive effect (β = 0.323, 95% HDI: 0.253 to 0.388), indicating that longer foreperiods speeded evidence accumulation. Relative to the uniform pretraining distribution, drift rate was lower in both the anti-exponential (β = − 0.142, 95% HDI: − 0.168 to − 0.118) and exponential (β = − 0.097, 95% HDI: − 0.121 to − 0.073) pretraining groups (Fig. 4b). The interaction between FP and pretraining distribution was credible for the anti-exponential condition (β = − 0.137, 95% HDI: − 0.242 to − 0.033), indicating that the FP effect on drift rate was attenuated following anti-exponential pretraining. For the exponential condition, the interaction was not credible (β = − 0.067, 95% HDI: − 0.167 to 0.030), suggesting that the FP effect on drift rate was comparable between the uniform and exponential pretraining groups.

For threshold, the current FP had a credible negative effect (β = − 0.446, 95% HDI: − 0.509 to − 0.385), reflecting reduced response caution with longer FPs. Relative to condition with uniform pretraining, threshold was lower in conditions with anti-exponential (β = − 0.123, 95% HDI: − 0.144 to − 0.099) and exponential (β = − 0.151, 95% HDI: − 0.173 to − 0.131) pretraining. The interaction between current FP and anti-exponential pretraining was not credible (β = − 0.093, 95% HDI: − 0.190 to 0.002), suggesting that the FP-dependent reduction in threshold did not differ reliably between conditions with uniform and anti-exponential pretraining (Fig. 4c). The interaction with exponential pretraining was also not credible (β = 0.017, 95% HDI: − 0.074 to 0.109), indicating that the FP effect on threshold was not sensitive to pretraining distribution.

As what is observed with the distribution effect model, the pattern of transfer effect could be predicted by model (Fig. 4d), which confirm that both drift rate and threshold have contributed in emergence of transfer effect. These parameter-level results specify how pretraining distribution exerts its transfer effect. Both anti-exponential and exponential pretraining reduced baseline drift rate and threshold relative to uniform, but the interaction patterns differed: anti-exponential pretraining attenuated the FP effect on drift rate, while exponential pretraining left the FP effects largely unchanged. For threshold, pretraining distribution lowered baseline levels without reliably modulating the FP effect. This suggests that different pretraining distributions produce distinct patterns of transfer at the decision level.

4. Discussion

This study provides the first comprehensive examination of the full family of temporal preparation effects in rats within a single paradigm, and the first application of the shifted Wald model to decompose these effects into latent cognitive components. Four main findings emerged. First, rats showed a robust current-trial FP effect, driven by both a reduction in decision threshold and an increase in drift rate. Second, sequential effects were weak and confined to threshold. Third, FP distribution systematically modulated both parameters: anti-exponential produced slower drift and lower threshold, while exponential reduced threshold without affecting drift. Fourth, a transfer effect emerged: exponential pretraining attenuated the RT–FP slope, while anti-exponential pretraining reduced baseline drift without modulating the FP slope. Together, these findings establish that rats exhibit a subset of the temporal preparation effects documented in humans, with the computational locus distributed across both decision-related parameters.

The robust current-trial FP effect is consistent with known effect in humans (Los, 2010; Niemi & Näätänen, 1981; Salet, Kruijne, van Rijn, et al., 2022), monkeys (Borzadaran et al., 2025; Brulé et al., 2021; de Hemptinne et al., 2007; Ilhame et al., 2015; Janssen & Shadlen, 2005; Oláh et al., 2020; Pasquereau & Turner, 2015; Tsuchiya et al., 2025), and extends rodent work demonstrating the basic variable FP effect (Davis et al., 2016; Hauber et al., 2001; Narayanan et al., 2006; O'Neill & Brown, 2007). The computational decomposition, however, provides a more nuanced picture. In humans, temporal expectation in fixed-FP and cueing paradigms has been primarily linked to non-decision processes (Jepma et al., 2012), with some studies suggested earlier onset of evidence accumulation (Bausenhart et al., 2010; Seibold et al., 2011), and improved accumulation rate as a function of temporal expectation (Rohenkohl et al., 2012). Also, impaired temporal prediction in Parkinson patients has been attributed to less flexible decision threshold adjustment in response to temporal predictability manipulations (Tomassini et al., 2019). Therefore, our findings reveal both shared and distinct pattern of temporal preparation effect on decision parameters with those observed with various paradigms in human. In the present study, the non-decision time parameter could not be reliably estimated when allowed to vary with FP, so we could not directly test whether temporal expectation in rats also modulates non-decision processes.

The reduction in decision threshold with longer FPs is supported by a study indicated that increasing target predictability improve motion detection through adjustments of the response criterion, not to changes in perceptual sensitivity (Katzner et al., 2012). A rise-to-threshold model indicated threshold adjustments rather than changes in information accumulation as the source of reaction time adjustment. Similarly, monkeys performing a vibrotactile detection task with variable stimulation times show response criterion modulation over the course of a trial (Carnevale et al., 2015). Premotor cortex population dynamics encoded this modulation, and a trained recurrent network model demonstrated a neural mechanism by which previous knowledge about the probability of stimulation over time can be intrinsically encoded to allow flexible control of the response criterion. A drift-diffusion analysis of an olfactory working memory task in mice revealed that earlier reward arrival lowered the decision bound (Reuschenbach et al., 2023). In the current task as FP grows the reward moments approaches and therefore decision criterion can be adjusted in a within trial time course. Together, these findings establish that temporal expectancy can adjust the decision criterion across species and paradigms. Such adjustment is consistent with a prediction of fMTP, where the dynamics of inhibition (I) and activation (A) over the foreperiod yield a decreasing I/A ratio as the FP lengthens; this increased preparation is proposed to lower the decision threshold, thereby providing a formal mechanism by which associative memory traces translate into criterion shifts (Salet, Kruijne, van Rijn, et al., 2022).

The simultaneous increase in drift rate suggests that temporal preparation also enhances the efficiency of evidence accumulation. Evidence that temporal expectation can improve the signal-to-noise ratio of sensory evidence comes from visual detection tasks in human (Cravo et al., 2013; Rohenkohl et al., 2012), where rhythmic temporal expectation enhanced the contrast sensitivity of targets, and a diffusion model indicated that this reflected an increased signal-to-noise gain of the sensory evidence upon which decisions were made. Speed pressure—a manipulation conceptually related to temporal urgency—has been shown to manifest in higher baseline firing rates of neurons that track the developing decision

process, as well as in a time-dependent increase in firing rates indicative of a growing urgency signal (Murphy et al., 2016). Computational analyses indicate that modulation of neural processing gain is a plausible mechanism for generating such urgency in decision circuits. Such urgency signal might be expressed as increased drift rate by growing FP in current study in rat, where reward maximization is the priority (Chakravarty et al., 2024) and speed pressure is intrinsic given the self-paced nature of task which require active holding of nosepoke throughout FP. These findings suggest that temporal expectancy can operate on multiple stages of the decision process, enhancing both the criterion for commitment and the quality of the evidence signal. This might be consistent with the idea that temporal expectation can affect both perception and action depending on whether accuracy or speed is priority (McCone, 2025; van Ede et al., 2020).

The present study could not address the role of non-decision time due to identifiability constraints. This is a notable limitation given that the human literature has often implicated non-decision processes as the primary locus of temporal expectation effects (Jepma et al., 2012). However, the observation that both threshold and drift rate are modulated in rats suggests that the computational architecture of temporal preparation may differ across species, or the shifted Wald model is not optimal for capturing pattern of reaction time in rat with voluntary component of FP.

The sequential effect current study was weak and largely confined to the decision threshold (Fig. …). Behaviorally, RT were generally slower when the history FP was long, and the slope of the FP–RT function was exaggerated with increasing history FP. At the decision level, the previous trial's FP had a small but credible positive effect on threshold, suggesting that response caution increased with increasing FP in the preceding trial. There was no credible effect on drift rate and no credible current × history interaction for either parameter. This contrasts with the robust asymmetric sequential effects typically observed in humans, where RT increases when the current FP is shorter than the preceding FP but is relatively unchanged when it is longer (Capizzi et al., 2015; Los, 2010). The weak sequential effect is notable but not unprecedented in non-human animals. In monkeys, the sequential effect was lacking in an arm-reaching task (Pasquereau & Turner, 2015), and in a stop-signal task its influence was context-dependent, affecting primarily response inhibition rather than simple RTs (Borzadaran et al., 2025).

Several explanations for the weak effect are plausible. The self-paced design with a relatively long 3 s inter-trial interval (ITI) may have minimized trial-to-trial carryover, as sequential effects are attenuated with longer ITIs in humans (Vallesi et al., 2013). The four FP durations (200–800 ms) were also relatively short; sequential effects may be more pronounced with longer FPs where the contrast between short and long is greater (Han & Proctor, 2022a, 2022b). Alternatively, the effect may reflect a genuine species difference in short-term temporal memory, consistent with the finding that sequential effects in macaques were largely independent of FP sequence in a stop-signal task (Borzadaran et al., 2025). Future studies systematically varying ITI and the nature of the warning signal would help distinguish these possibilities.

One methodological feature of our task may be particularly relevant: the self-paced design required both voluntary initiation of the FP (via nose-poke entry) and active waiting (maintaining nose position in the aperture throughout the FP). This contrasts with typical experimenter-paced designs where the warning signal is externally presented and the FP is imposed without a concurrent motor requirement. Recent evidence suggests that voluntary actions interact with temporal preparation. It has recently been indicated that RT were slower for self-initiated than externally initiated stimuli, particularly at shorter FPs, and that this effect was observed only in variable-FP experiments (Nobre et al., 2026). This raises the possibility that in our self-paced design, the animal's own preparatory state may have dominated the preparation process, reducing the influence of trial history. Additionally, the requirement for active waiting engaged sustained motor inhibition (Narayanan et al., 2006), which may have altered the balance between inhibitory and excitatory processes thought to shape sequential effects (Salet, Kruijne, van Rijn, et al., 2022). These considerations suggest that the weak sequential effect may partly reflect the self-paced, active-waiting nature of the task rather than a species difference alone.

The finding that threshold, but not drift rate, was modulated by the previous trial's FP is theoretically informative. It suggests that trial history influences the animal's response criterion—perhaps through carryover of preparatory activation or inhibition—without affecting the efficiency of evidence accumulation. This is broadly consistent with memory-based accounts, which posit that memory traces from previous trials influence preparation on subsequent trials (Los et al., 2014; Salet, Kruijne, van Rijn, et al., 2022). However, if memory traces accumulate and jointly determine performance, sequential effects should be more robust. One possibility is that memory traces in rats, decay more rapidly than in humans, or that in highly trained animals, temporal preparation depends heavily on general statistics of FP across previous trials rather than on recency of memory traces (Borzadaran et al., 2025). Another possibility is that the self-paced design shifts the balance between inhibition and activation processes that shape the sequential effect (Salet, Kruijne, van Rijn, et al., 2022). This dissociation between the current trial effect (both parameters) and the sequential effect (threshold only) suggests that different temporal preparation mechanisms may operate on different timescales, with trial-history effects being less effective than within-trial preparation.

The distribution of FPs modulated both overall RT and the shape of the RT–FP function. Anti-exponential produced slightly slower overall responses than uniform, while exponential produced faster overall responses. Both non-uniform distributions flattened the RT–FP slope relative to uniform, with a stronger flattening for anti-exponential. Notably, this pattern diverges from human findings, where anti-exponential typically steepens the RT–FP function and exponential flatten it, indicating comparable temporal preparation across FPs (Los et al., 2014; Los et al., 2017). Hazard-based models (Janssen & Shadlen, 2005; Nobre et al., 2007) predict a flat RT–FP function under exponential distribution because the hazard rate is constant. In rats, the exponential RT–FP function was not flat—it retained a clear negative slope—so the hazard-based prediction fails to account the pattern of RT-FP function. Moreover, the anti-exponential distribution, which produces a steeply rising hazard function, did not steepen the RT–FP slope as hazard-based models predict. Memory-based accounts predict that accumulated traces of experienced FPs produce both distribution effects and asymmetric sequential effects (Los et al.,

2014; Los et al., 2017; Los et al., 2021; Salet, Kruijne, van Rijn, et al., 2022). The weak sequential effects in rats, together with generally comparable RT–FP functions across distributions, contradict this prediction. The fMTP framework (Salet, Kruijne, van Rijn, et al., 2022) captures human distribution and sequential effects, but its assumptions about trial-history-based memory traces do not align with the present rat data.

At the decision level, anti-exponential reduced drift rate and attenuated the FP effect on drift, whereas exponential reduced threshold without affecting drift or its modulation by FP. Both non-uniform distributions lowered threshold relative to uniform. Thus, different aspects of the distribution selectively engaged different decision components. The general threshold reduction across both non-uniform distributions may reflect an adjustment of response caution to temporal uncertainty. A uniform distribution over FPs has maximum Shannon entropy, whereas non-uniform distributions reduce entropy by making one FP more probable. If the decision threshold is adjusted to the precision of temporal predictions, a more predictable FP structure should lower the criterion for committing to a response (Vossel et al., 2014). This account aligns with evidence that temporal expectation primarily affects the decision criterion rather than sensory sensitivity (Katzner et al., 2012; Lawlor et al., 2023) and with neurophysiological findings that premotor cortex dynamically encodes the response criterion under temporal uncertainty (Carnevale et al., 2015). In contrast, the selective attenuation of the FP effect on drift under anti-exponential distribution suggests that the shape of the distribution specifically modulates the efficiency of evidence accumulation, possibly through memory traces that shape the activation/inhibition balance across FP range (Los et al., 2017; Salet, Kruijne, van Rijn, et al., 2022).

None of hazard-based or memory-based accounts cannot account for full picture of distribution effects in the current study. One possibility may be that the self-paced design—requiring voluntary initiation of the FP and active waiting by holding the nose poke—fundamentally alters the preparatory state compared with experimenter-paced paradigms. In such a design, preparation may be dominated by endogenous motor signals tied to the animal's own action, rather than by the statistical structure of the FP distribution or by retrieval of past memory traces. This could explain why the RT–FP functions remained largely parallel across distributions and why sequential effects were weak. Recent human work shows that voluntary actions interact with temporal preparation (Nobre et al., 2026). Therefore, the distribution effects observed in the current study may reflect a preparatory regime in which voluntary motor control plays a more prominent role than in typical human experiments.

The transfer effect was observed at the behavioral level (attenuation of the RT–FP slope following exponential pretraining) and was accompanied by parameter-level changes in both drift and threshold. Both anti-exponential and exponential pretraining reduced baseline drift and threshold relative to uniform, but interaction patterns differed: anti-exponential pretraining attenuated the FP effect on drift, while exponential pretraining left FP effects largely unchanged for drift but attenuated the RT–FP slope at the behavioral level.

The transfer pattern is a direct reproduction of the distribution effect, which suggests a common mechanism. The parameter-level changes in the test phase map closely onto those observed during pretraining itself. In the distribution experiment, anti-exponential reduced drift rate and attenuated the FP effect on drift, while exponential lowered threshold without affecting drift. In the transfer experiment, the same signatures reappeared. This mirroring is theoretically informative: it suggests that the distribution effect is not a transient adjustment to the current context, but leaves a lasting imprint on the decision parameters. The most parsimonious explanation is that the same automatic mechanism underlies both effects, and that this mechanism persists into the test phase.

This carryover is a core prediction of the fMTP (Salet, Kruijne, van Rijn, et al., 2022), which posits that temporal preparation is driven by associative learning: each trial leaves a memory trace, and these traces are automatically retrieved by the warning stimulus to jointly determine the preparatory state. This framework explains phenomena across multiple time scales, from fast sequential effects to long-term memory effects over weeks, by assuming that traces are accumulated and forgotten according to associative learning principles. The transfer effect we observed—where the pretraining distribution's influence persists across an entire testing session—fits naturally within this framework. The pretraining phase creates a set of strong, accumulated memory traces that are automatically retrieved in the test phase, biasing the decision parameters (drift and threshold) in the direction established during pretraining.

The persistence of this carryover is notable given how rapidly rodents update timed behavior. Rats and mice can adjust their responses in fixed-interval task within 2–3 trials of an interval change. If temporal expectations are updated this quickly, the persistence of the transfer effect across an entire testing session implies that the pretraining memory traces are not rapidly overwritten by online adaptation. This is consistent with the fMTP framework's assumption of a recency-weighted forgetting mechanism, where traces decay slowly, allowing their influence to persist even as the animal adapts to the new distribution. Purely hazard-based accounts (Janssen & Shadlen, 2005; Nobre et al., 2007), which predict rapid adaptation to the new uniform testing distribution, cannot easily accommodate this carryover. This finding aligns with the idea that temporal preparation is driven by past experience, not by the current hazard function (Los et al., 2017). Together, the distribution and transfer effects suggest a two-level temporal preparation system: fast, online tracking of the current FP distribution, and slower, cumulative memory traces that bias the decision parameters over longer timescales. The fMTP framework provides a unified account of this system, where the same associative learning process operates across these different time scales

Despite the novel insights provided by this study, several limitations warrant consideration. First, the non-decision time parameter could not be reliably estimated when allowed to vary with FP, as revealed by our parameter recovery simulations, and others (Salet, Kruijne, van Rijn, et al., 2022). This identifiability constraint prevented us from directly testing whether temporal preparation in rats modulates non-decision processes (e.g., sensory encoding or motor preparation), which have been frequently implicated in human studies (Jepma et al., 2012). Future studies employing experimenter-based FPs along with

discrimination tasks might better fit to examine role of non-decision time in temporal preparation effects. Second, the sequential effect was notably weaker than typically observed in humans, and our task design may have contributed to this. The self-paced nature of the task, requiring voluntary initiation of the FP through nose-poke entry and active waiting throughout the FP, may have engaged sustained motor inhibition that altered the balance of preparatory processes during FP. Additionally, the relatively long inter-trial interval (3 s) and the narrow range of FP durations (200–800 ms) may have limited the emergence of robust sequential effects, which are sensitive to these parameters (Han & Proctor, 2022a; Vallesi et al., 2013). Third, our sample size (N = 10 after exclusions) was modest, and although Bayesian methods are robust with small samples, future studies with larger cohorts could increase precision and allow for individual differences analyses. Finally, the transfer effects observed here were assessed within a single test session immediately following acquisition; whether these effects persist over longer delays or generalize across contexts remains unknown. Future studies should examine the durability and boundary conditions of transfer effects, as well as their neural substrates using the powerful circuit-manipulation tools available in rodents.

In conclusion, this study provides the first comprehensive demonstration that rats exhibit multiple temporal preparation effects within a single variable FP paradigm, with computational mechanisms that can be dissected using the shifted Wald model. The current-trial FP effect was robust and driven by dual modulation of decision threshold and drift rate, suggesting that temporal expectation influences both response caution and the efficiency of evidence accumulation. Distribution and transfer effects were parameter-specific, with anti-exponential distributions selectively reducing drift rate and exponential distributions reducing threshold, patterns that carried over into subsequent test phases. These findings establish the rat as a valuable translational model for studying temporal preparation and reveal both conserved and potentially species-specific aspects of its computational architecture. Importantly, the observation that temporal preparation in rats engages decision-related parameters (threshold and drift rate) rather than solely non-decision processes—as often emphasized in human literature—suggests that the locus of temporal preparation effects may depend on task demands, species-specific constraints, or both.

Declarations

Additional information

Competing interests:

The author(s) declare no competing interests.

Funding

This work was supported by the Neuroscience Research Center of Kerman University of Medical Sciences.

Author Contribution

Fatemeh Mafi: investigation; writing – original draft; formal analysis. Mohammad Reza Afarinesh: writing – review and editing. Vahid Sheibani: writing – review and editing. Sadegh Ghasemian: conceptualization; formal analysis; writing – review and editing.

Acknowledgement

This work was supported by the Neuroscience Research Center of Kerman University of Medical Sciences. DeepSeek (accessed September 2026) was used for language editing, manuscript refinement, and analytic scripting support.

Data Availability

All analysis scripts and processed data supporting this study are available at https://github.com/SadeghGhasemian/TP-rat.

References

1. Albus, U. *Guide for the care and use of laboratory animals* 8th edn (In: Sage Publications Sage UK, 2012).
2. Anders, R., Alario, F. & Van Maanen, L. The shifted Wald distribution for response time data analysis. *Psychol. Methods*. **21** (3), 309 (2016).
3. Bausenhart, K. M., Rolke, B., Seibold, V. C. & Ulrich, R. Temporal preparation influences the dynamics of information processing: Evidence for early onset of information accumulation. *Vision. Res.* **50** (11), 1025–1034. https://doi.org/https://doi.org/10.1016/j.visres.2010.03.011 (2010).
4. Bausenhart, K. M. M. & Ulrich, R. What is prepared in temporal preparation? A review and a historical appreciation [Review]. *Frontiers in Psychology*, *Volume 17–2026*. (2026). https://doi.org/10.3389/fpsyg.2026.1768431
5. Borzadaran, F. M. et al. Temporal Preparation and Executive Functions in the Context of a Variable Foreperiod Stop-Signal Paradigm in Macaque Monkey: Evidence From Bayesian Parametric Approach. *Am. J. Primatol.* **87** (12), e70101 (2025).
6. Brulé, S., Herlin, B., Pouget, P. & Missal, M. Ketamine reduces temporal expectation in the rhesus monkey. *Psychopharmacology* **238** (2), 559–567 (2021).
7. Capizzi, M., Correa, Á., Wojtowicz, A. & Rafal, R. D. Foreperiod priming in temporal preparation: Testing current models of sequential effects. *Cognition* **134**, 39–49 (2015).
8. Carnevale, F., de Lafuente, V., Romo, R., Barak, O. & Parga, N. Dynamic control of response criterion in premotor cortex during perceptual detection under temporal uncertainty. *Neuron* **86** (4), 1067–1077

(2015).

9. Chakravarty, S. et al. A cross-species framework for investigating perceptual evidence accumulation. *bioRxiv*, 2024.2004. 2017.589945. (2024).
10. Cravo, A. M., Rohenkohl, G., Wyart, V. & Nobre, A. C. Temporal Expectation Enhances Contrast Sensitivity by Phase Entrainment of Low-Frequency Oscillations in Visual Cortex. *J. Neurosci.* **33** (9), 4002. https://doi.org/10.1523/JNEUROSCI.4675-12.2013 (2013).
11. Crowe, E. M., Los, S. A., Schindler, L. & Kent, C. Transfer effects in auditory temporal preparation occur using an unfilled but not filled foreperiod. *Q. J. Experimental Psychol.* **74** (8), 1432–1438 (2021).
12. Davis, C. M., Roma, P. G. & Hienz, R. D. The rodent Psychomotor Vigilance Test (rPVT): a method for assessing neurobehavioral performance in rats and mice. *JoVE (Journal Visualized Experiments)* (118), e54629. (2016).
13. de Hemptinne, C., Nozaradan, S., Duvivier, Q., Lefevre, P. & Missal, M. How do primates anticipate uncertain future events? *J. Neurosci.* **27** (16), 4334–4341 (2007).
14. Han, T. & Proctor, R. W. Change of Variable-Foreperiod Effects within an Experiment: A Bayesian Modeling Approach. *J. Cognition*. **5** (1), 40–40. https://doi.org/10.5334/joc.235 (2022a).
15. Han, T. & Proctor, R. W. Revisiting variable-foreperiod effects: evaluating the repetition priming account. *Atten. Percept. Psychophys.* **84** (4), 1193–1207. https://doi.org/10.3758/s13414-022-02476-5 (2022b).
16. Hauber, W., Giertler, C. & Bohn, I. NMDA and dopamine D2 receptors in the caudate-putamen are not involved in control of motor readiness in rats. *Psychopharmacology* **155** (1), 43–51. https://doi.org/10.1007/s002130000663 (2001).
17. Heathcote, A. Fitting Wald and ex-Wald distributions to response time data: An example using functions for the S-PLUS package. *Behav. Res. Methods Instruments Computers*. **36** (4), 678–694 (2004).
18. Ilhame, A., Nicolas, W., Pierre, P. & Marcus, M. A subanesthetic dose of ketamine in the Rhesus monkey reduces the occurrence of anticipatory saccades. *Psychopharmacology* **232** (19), 3563–3572 (2015).
19. Janssen, P. & Shadlen, M. N. A representation of the hazard rate of elapsed time in macaque area LIP. *Nat. Neurosci.* **8** (2), 234–241. https://doi.org/10.1038/nn1386 (2005).
20. Jepma, M., Wagenmakers, E. J. & Nieuwenhuis, S. Temporal expectation and information processing: A model-based analysis. *Cognition* **122** (3), 426–441. https://doi.org/https://doi.org/10.1016/j.cognition.2011.11.014 (2012).
21. Katzner, S., Treue, S. & Busse, L. Improving behavioral performance under full attention by adjusting response criteria to changes in stimulus predictability. *J. Vis.* **12** (10), 1–1. https://doi.org/10.1167/12.10.1 (2012).
22. Lawlor, J., Zagala, A., Jamali, S. & Boubenec, Y. Pupillary dynamics reflect the impact of temporal expectation on detection strategy. *Iscience*, **26**(2). (2023).

23. Leth-Steensen, C. Lengthening fixed preparatory foreperiod durations within a digit magnitude classification task serves mainly to shift distributions of response times upwards. *Acta. Psychol.* **130** (1), 72–80. https://doi.org/https://doi.org/10.1016/j.actpsy.2008.10.003 (2009).
24. Los, S. A. Foreperiod and sequential effects: Theory and data. *Atten. time*. **289** (302), 24 (2010).
25. Los, S. A., Kruijne, W. & Meeter, M. Outlines of a multiple trace theory of temporal preparation [Review]. *Frontiers in Psychology*, *Volume 5–2014*. (2014). https://doi.org/10.3389/fpsyg.2014.01058
26. Los, S. A., Kruijne, W. & Meeter, M. Hazard versus history: Temporal preparation is driven by past experience. *J. Exp. Psychol. Hum. Percept. Perform.* **43** (1), 78 (2017).
27. Los, S. A. et al. The warning stimulus as retrieval cue: The role of associative memory in temporal preparation. *Cogn. Psychol.* **125**, 101378 (2021).
28. Mattiesing, R. M., Kruijne, W., Meeter, M. & Los, S. A. Timing a week later: The role of long-term memory in temporal preparation. *Psychon. Bull. Rev.* **24** (6), 1900–1905 (2017).
29. Matzke, D. & Wagenmakers, E. J. Psychological interpretation of the ex-Gaussian and shifted Wald parameters: A diffusion model analysis. *Psychon. Bull. Rev.* **16** (5), 798–817 (2009).
30. McCone, H. *Time is of the Essence: The Dynamic Interplay Between Timing and Evidence Accumulation in Perceptual Decision Making* (University of Dublin, 2025).
31. Murphy, P. R., Boonstra, E. & Nieuwenhuis, S. Global gain modulation generates time-dependent urgency during perceptual choice in humans. *Nat. Commun.* **7** (1), 13526. https://doi.org/10.1038/ncomms13526 (2016).
32. Narayanan, N. S., Horst, N. K. & Laubach, M. Reversible inactivations of rat medial prefrontal cortex impair the ability to wait for a stimulus. *Neuroscience* **139** (3), 865–876. https://doi.org/https://doi.org/10.1016/j.neuroscience.2005.11.072 (2006).
33. Niemi, P. & Näätänen, R. Foreperiod and simple reaction time. *Psychol. Bull.* **89** (1), 133 (1981).
34. Nobre, A. C., Correa, A. & Coull, J. T. The hazards of time. *Curr. Opin. Neurobiol.* **17** (4), 465–470. https://doi.org/https://doi.org/10.1016/j.conb.2007.07.006 (2007).
35. Nobre, A. P., Paris-Colombo, G., Claessens, P. M. E. & Cravo, A. M. The influence of voluntary actions on temporal preparation to visual stimuli. *J. Exp. Psychol. Hum. Percept. Perform.* **52** (1), 57 (2026).
36. O'Neill, M. & Brown, V. J. Amphetamine and the adenosine A2a antagonist KW-6002 enhance the effects of conditional temporal probability of a stimulus in rats. *Behav. Neurosci.* **121** (3), 535 (2007).
37. Oláh, V., Knakker, B., Trunk, A., Lendvai, B. & Hernádi, I. Dissociating cholinergic influence on alertness and temporal attention in primates in a simple reaction time paradigm. *Eur. J. Neurosci.* **52** (7), 3776–3789 (2020).
38. Pasquereau, B. & Turner, R. S. Dopamine neurons encode errors in predicting movement trigger occurrence. *J. Neurophysiol.* **113** (4), 1110–1123. https://doi.org/10.1152/jn.00401.2014 (2015).

39. Reuschenbach, J., Reinert, J. K., Fu, X. & Fukunaga, I. Effects of Stimulus Timing on the Acquisition of an Olfactory Working Memory Task in Head-Fixed Mice. *J. Neurosci.* **43** (17), 3120. https://doi.org/10.1523/JNEUROSCI.1636-22.2023 (2023).
40. Rohenkohl, G., Cravo, A. M., Wyart, V. & Nobre, A. C. Temporal Expectation Improves the Quality of Sensory Information. *J. Neurosci.* **32** (24), 8424. https://doi.org/10.1523/JNEUROSCI.0804-12.2012 (2012).
41. Salet, J. It's About Time: computational and Experimental Investigations of Adaptation to Nature's Temporal Structure. (2023).
42. Salet, J. M., Kruijne, W., Rijn, H., Zimmermann, E. & Schlichting, N. Temporal Preparation and Statistical Learning: The Influence of Temporal Preparation on Statistical Learning Effects in Complex Temporal Environments. *bioRxiv*, 2022.2008. 2006.502990. (2022).
43. Salet, J. M., Kruijne, W., van Rijn, H., Los, S. A. & Meeter, M. FMTP: A unifying computational framework of temporal preparation across time scales. *Psychol. Rev.* **129** (5), 911 (2022).
44. Seibold, V. C., Bausenhart, K. M., Rolke, B. & Ulrich, R. Does temporal preparation increase the rate of sensory information accumulation? *Acta. Psychol.* **137** (1), 56–64 (2011).
45. Shdeour, O., Tal-Perry, N., Glickman, M. & Yuval-Greenberg, S. Exposure to temporal variability promotes subsequent adaptation to new temporal regularities. *Cognition* **244**, 105695. https://doi.org/https://doi.org/10.1016/j.cognition.2023.105695 (2024).
46. Tomassini, A., Pollak, T. A., Edwards, M. J. & Bestmann, S. Learning from the past and expecting the future in Parkinsonism: Dopaminergic influence on predictions about the timing of future events. *Neuropsychologia* **127**, 9–18. https://doi.org/https://doi.org/10.1016/j.neuropsychologia.2019.02.003 (2019).
47. Tsuchiya, T. et al. Cognitive effects of scopolamine on temporal preparation in male macaque monkeys. *Behav. Brain. Res.* **489**, 115599. https://doi.org/https://doi.org/10.1016/j.bbr.2025.115599 (2025).
48. Tsunoda, Y. & Kakei, S. Reaction time changes with the hazard rate for a behaviorally relevant event when monkeys perform a delayed wrist movement task. *Neurosci. Lett.* **433** (2), 152–157. https://doi.org/https://doi.org/10.1016/j.neulet.2007.12.063 (2008).
49. Vallesi, A., Lozano, V. N. & Correa, Á. Dissociating temporal preparation processes as a function of the inter-trial interval duration. *Cognition* **127** (1), 22–30 (2013).
50. van den Brink, R. L., Murphy, P. R., Desender, K., de Ru, N. & Nieuwenhuis, S. Temporal Expectation Hastens Decision Onset But Does Not Affect Evidence Quality. *J. Neurosci.* **41** (1), 130. https://doi.org/10.1523/JNEUROSCI.1103-20.2020 (2021).
51. van Ede, F., Rohenkohl, G., Gould, I. & Nobre, A. C. Purpose-Dependent Consequences of Temporal Expectations Serving Perception and Action. *J. Neurosci.* **40** (41), 7877. https://doi.org/10.1523/JNEUROSCI.1134-20.2020 (2020).
52. Vangkilde, S., Petersen, A. & Bundesen, C. Temporal expectancy in the context of a theory of visual attention. *Philos. Trans. R Soc. Lond. B Biol. Sci.* **368** (1628), 20130054.

https://doi.org/10.1098/rstb.2013.0054 (2013).

53. Vossel, S. et al. Spatial attention, precision, and Bayesian inference: a study of saccadic response speed. *Cereb. Cortex*. **24** (6), 1436–1450 (2014).
54. Xiong, Z., Job, X. & Kilteni, K. Costs and benefits of temporal expectations on somatosensory perception and decision-making. *Cognition* **261**, 106146. https://doi.org/https://doi.org/10.1016/j.cognition.2025.106146 (2025).

Figures

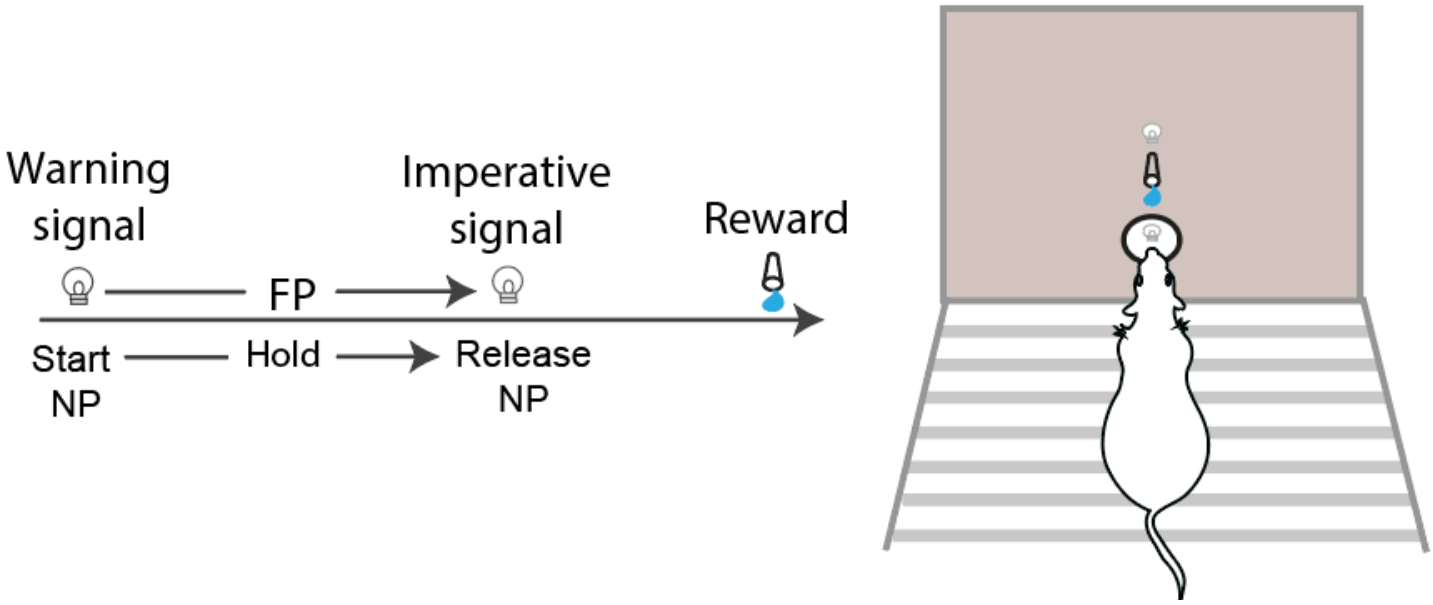

Figure 1

Schematic illustration of the apparatus and task events. At the start of each trial, a white LED behind the transparent rear wall of the nose-poke (NP) aperture served as the warning signal. Upon nose entry into the aperture, the LED was turned off and the foreperiod (FP) began. During the FP, rats were required to maintain their nose in the aperture. The FP ended with illumination of the LED above the NP aperture, which served as the imperative signal. Rats then had to withdraw from the NP aperture and lick the spout above it (as response) and take the reward.

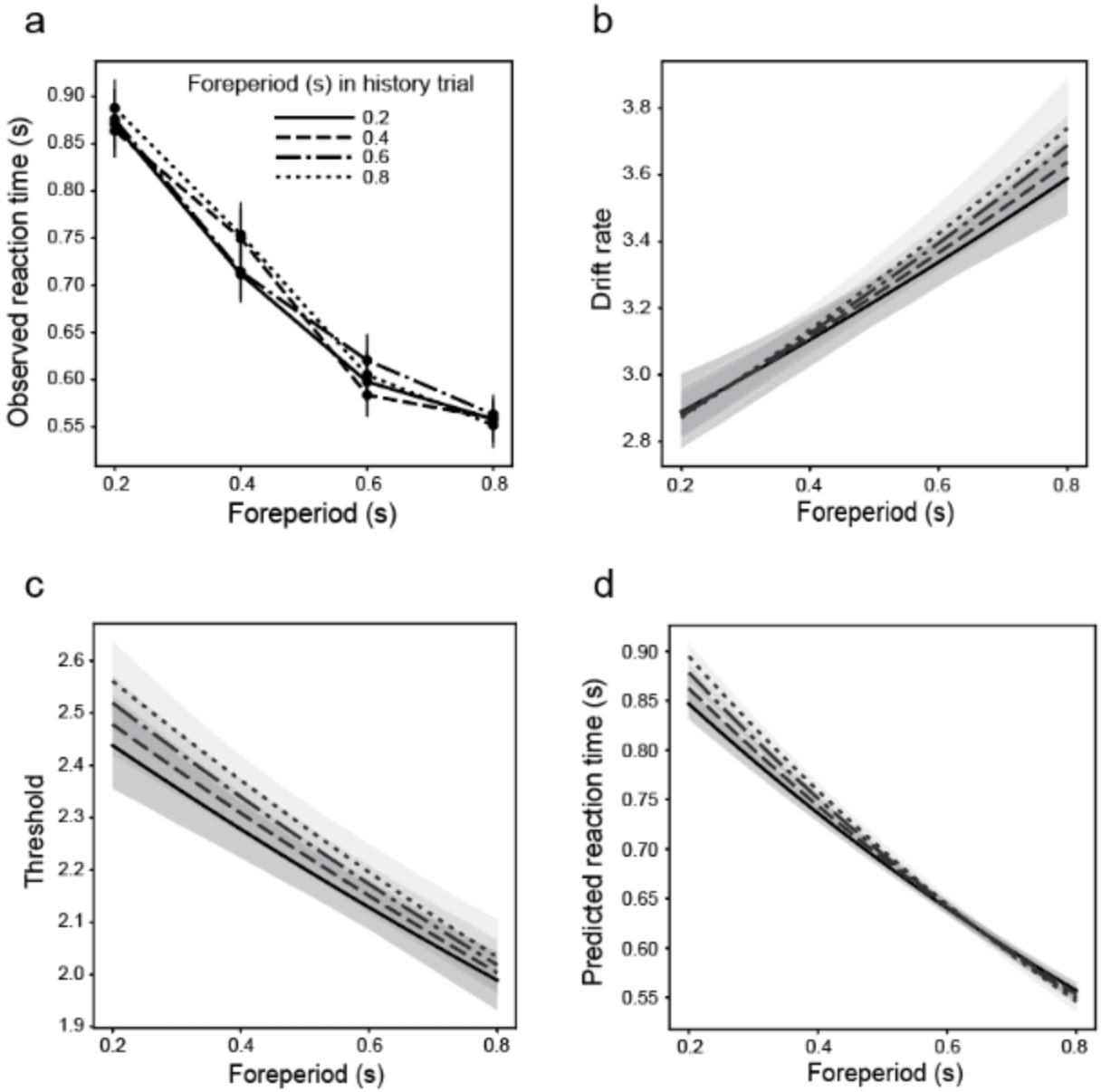

Figure 2

Sequential effect in observed reaction time and shifted Wald parameters. (a) Observed mean reaction time (± SEM) as a function of current foreperiod, separately for each history foreperiod. (b) Posterior means of drift rate as a function of current foreperiod for trials with different history foreperiods. (c) Posterior means of decision threshold as a function of current foreperiod for trials with different history foreperiods. (d) Model-predicted reaction time ($\alpha/\gamma + \theta$) as a function of current foreperiod, separately for each history foreperiod. In panels b–d, shaded regions represent the 95% highest density interval (HDI) of the posterior distribution. Line styles in all panels denote the history foreperiod: solid = 0.2 s, dashed = 0.4 s, dash-dot = 0.6 s, dotted = 0.8 s.

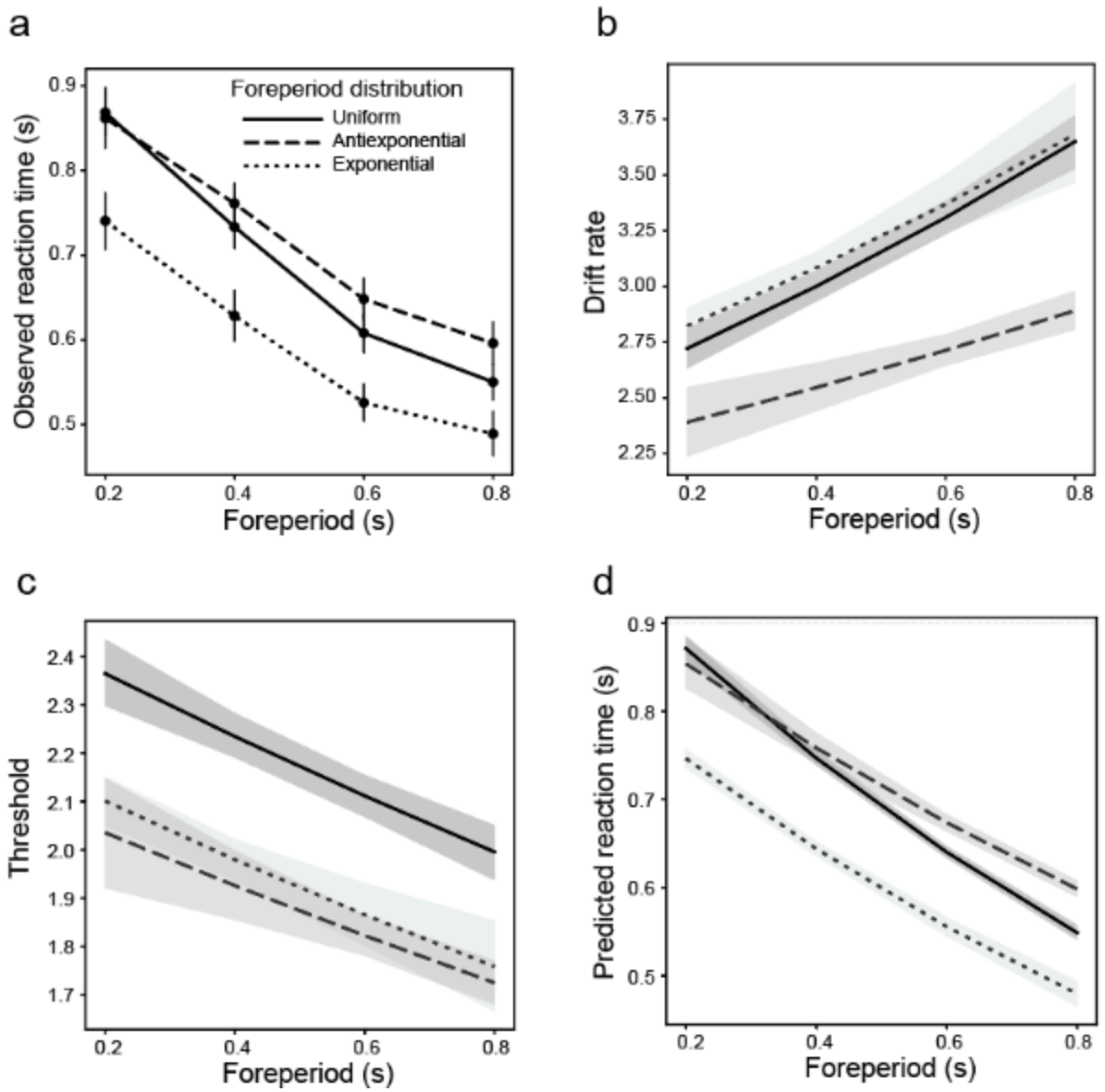

Figure 3

Effects of foreperiod distribution on observed reaction time and shifted Wald parameters. (a) Observed mean reaction time (± SEM) as a function of current foreperiod, separately for each foreperiod distribution (uniform, antiexponential, exponential). (b) Posterior means of drift rate as a function of current foreperiod for each distribution. (c) Posterior means of decision threshold as a function of current foreperiod for each distribution. (d) Model-predicted reaction times ($\alpha/\gamma + \theta$) as a function of current foreperiod, separately for each distribution. In panels b–d, shaded regions represent the 95% highest density interval (HDI) of the posterior distribution. Line styles in all panels denote the foreperiod distribution: solid = uniform, dashed = antiexponential, dotted = exponential.

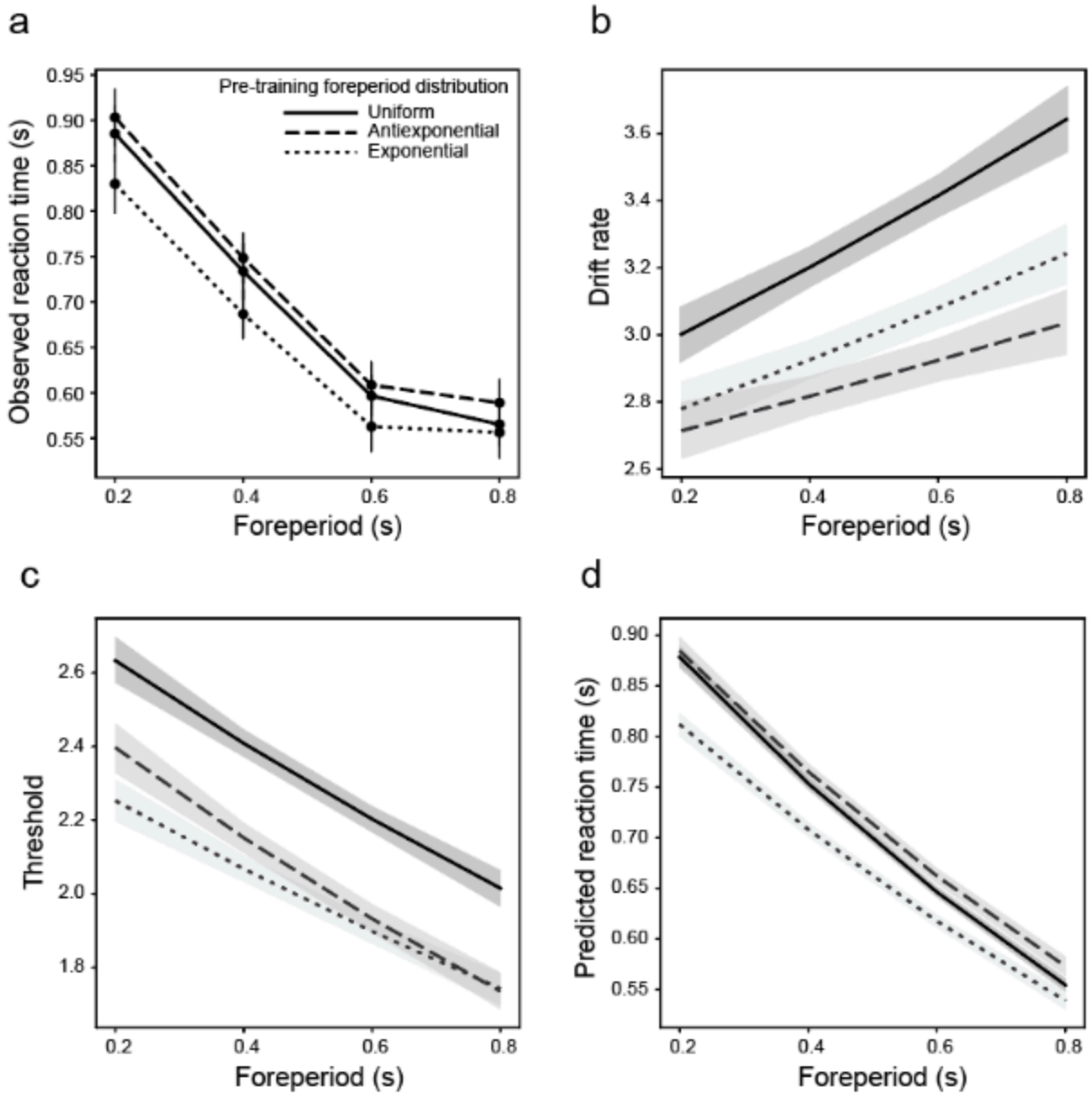

Figure 4

Transfer effect in observed reaction times and shifted Wald parameters. (a) Observed mean reaction time (± SEM) as a function of current foreperiod, separately for each pre-training foreperiod distribution. (b) Posterior means of drift rate as a function of current foreperiod for each pre-training foreperiod distribution. (c) Posterior means of decision threshold as a function of current foreperiod for each pre-training foreperiod distribution. (d) Model-predicted reaction times ($\alpha/\gamma + \theta$) as a function of current foreperiod, separately for each pre-training foreperiod distribution. The shaded areas represent the 95% highest density interval (HDI) of the posterior distributions. Line styles in all panels denote the pre-training foreperiod distribution: solid = uniform, dashed = antiexponential, dotted = exponential.

Supplementary Files

This is a list of supplementary files associated with this preprint. Click to download.

- Supplementarymaterials.pdf